THE ASTROPHYSICAL JOURNAL, 520:833–840, 1999 August 1

A SIMPLE SCALING ANALYSIS OF X-RAY EMISSION AND ABSORPTION IN HOT-STAR WINDS

STANLEY P. OWOCKI AND DAVID H. COHEN
Bartol Research Institute, University of Delaware, Newark, DE 19716; owocki@bartol.udel.edu, cohen@bartol.udel.edu
Received 1999 January 5; accepted 1999 March 11

ABSTRACT

We present a simple analysis of X-ray emission and absorption for hot-star winds, designed to explore the natural scalings of the observed X-ray luminosity with wind and stellar properties. We show that an exospheric approximation, in which all of the emission above the optical depth unity radius escapes the wind, reproduces very well the formal solution for radiation transport through a spherically symmetric wind. Using this approximation we find that the X-ray luminosity L_X scales naturally with the wind density parameter $\dot{M}/v_\infty$, obtaining $L_X \sim (\dot{M}/v_\infty)^2$ for optically thin winds, and $L_X \sim (\dot{M}/v_\infty)^{1+s}$ for optically thick winds with an X-ray filling factor that varies in radius as $f \sim r^s$. These scalings with wind density contrast with the commonly inferred empirical scalings of X-ray luminosity L_X with bolometric luminosity L_{Bol}. The empirically derived linear scaling of $L_X \sim L_{Bol}$ for thick winds can, however, be reproduced through a delicate cancellation of emission and absorption, if one assumes modest radial fall-off in the X-ray filling factor ($s \approx -0.25$ or $s \approx -0.4$, depending on details of the secondary scaling of wind density with luminosity). We also explore the nature of the X-ray spectral energy distribution in the context of this model and find that the spectrum is divided into a soft, optically thick part and a hard, optically thin part. Finally, we conclude that the energy-dependent emissivity must have a high-energy cutoff, corresponding to the maximum shock energy, in order to reproduce the general trends seen in X-ray spectral energy distributions of hot stars.

Subject headings: radiative transfer — shock waves — stars: early-type — stars: mass loss — stars: winds, outflows — X-rays: stars

1. INTRODUCTION

One of the great surprises of the *Einstein* X-ray satellite mission was the observation that hot, luminous, OB stars are strong emitters of soft ($\sim$1 keV) X-rays (Harnden et al. 1979; Seward et al. 1979). Unlike the cooler, late-type stars for which the X-ray emission was found to scale with the star's rotation, the observed X-rays from hot stars show a roughly linear proportionality to the stellar bolometric luminosity, $L_X \approx 10^{-7} L_{Bol}$ (Long & White 1980; Pallavicini et al. 1981; Chlebowski, Harnden, & Sciortino 1989). Observations from subsequent X-ray satellites, most notably *ROSAT*, have generally confirmed this earlier scaling result, with some minor refinements. For example, from a *ROSAT* survey of 42 O stars, Kudritzki et al. (1996) find $\log L_X/L_{Bol} \approx -6.7 \pm 0.35$, with a somewhat tighter relationship when a weak dependence on a characteristic wind density $\dot{M}/v_\infty$ is included, $L_X \propto (\dot{M}/v_\infty)^{-0.38} L_{Bol}^{1.34}$.

Even before these detections, X-ray emission from a narrow stellar "corona" was postulated to explain the superionization seen in the UV spectra of OB stars (Cassinelli & Olson 1979). This coronal model was further refined by Waldron (1984), but other studies have limited the extent, temperature, and fractional contribution of the total X-ray output of such purported O star coronae (Cassinelli, Olson, & Stalio 1978; Nordsieck, Cassinelli, & Anderson 1981; Cassinelli & Swank 1983; Baade & Lucy 1987; MacFarlane et al. 1993). A much more generally favored scenario has been that these X-rays arise from *shocks* that form in the wind from strong intrinsic instabilities in the line-driving mechanism (Lucy & Solomon 1970; MacGregor, Hartmann, & Raymond 1979; Owocki & Rybicki 1984, 1985). Lucy & White (1980) and Lucy (1982) proposed phenomenological models in which wind material accelerated by this line-driven instability rams into ambient, "shadowed" material, forming a *forward* shock that accelerates and heats that material, producing X-rays.

Dynamical simulation models of the nonlinear evolution of this instability have since indicated a quite different wind structure, dominated by *reverse* shocks that *decelerate* very rarefied, instability-accelerated material as it rams into compressed, dense shells ahead of it (Owocki, Castor, & Rybicki 1988). Since only a small fraction of wind material is actually heated by passage through such reverse shocks, the resulting direct X-ray emission is very low, generally well below the observed value (Feldmeier et al. 1997a). To overcome this limitation, subsequent wind structure simulations by Feldmeier, Puls, & Pauldrach (1997b) introduced a chaotic, turbulent perturbation at the photospheric lower boundary. This seeds a wind structure with substantial velocity dispersion among the dense shells, which thus collide among themselves, yielding much more shock-heated material. For the specific case of a massive OB supergiant wind with rather strong and chaotic base perturbations, the X-ray emission produced in such models can be made to approach the observed values. However, the dynamical simulations for particular cases have thus far made no attempt to explain the broad scaling of observed X-ray emission with stellar luminosity.

The goal of the present paper is to provide a firm basis for understanding these more general scaling properties of hot-star X-rays. Our approach here eschews detailed dynamical simulations and instead examines phenomenological models of the X-ray emission, in order to define more clearly what overall properties are needed from instability-generated wind structure simulations to produce these observed scaling relations. A major point of our analysis is that a *linear* scaling of *observed* L_X with L_{Bol} does not arise naturally from expected properties of a wind-shock model

but requires a rather delicate balance of X-ray absorption and emission, which in turn requires a special form for the radial distribution of wind shocks. A further point is that such a balance between emission and absorption should be associated with specific trends in broadband X-ray spectral properties.

The remainder of this paper is organized as follows: Beginning from the formal solution to the radiation transfer equation for X-rays emitted throughout an expanding stellar wind (§ 2.1), we develop a simple "exospheric" approximation through which we derive a general scaling law for X-ray luminosity from a simple power-law emission model (§ 2.2). By relating this to wind and stellar scaling laws we identify parameter requirements for reproducing the observationally inferred linear dependence of L_X on L_{Bol} (§ 2.3). We next examine the energy dependence of the X-ray spectrum (§ 3.1) and then integrate the expression for the X-ray spectrum over energy in order to verify the result from the previous section that gave the linear $L_X \sim L_{Bol}$ scaling (§ 3.2). The final section (§ 4) summarizes our conclusions. In Appendices A and B we examine the effect of assuming a constant wind velocity and verify the validity of the assumption of a smooth X-ray emissivity in terms of detailed numerical plasma emission models.

2. RADIATION TRANSFER THROUGH AN EXPANDING, SPHERICAL STELLAR WIND

2.1. *Formal Solution for Constant Velocity Expansion*

To develop a simplified description of X-ray emission and absorption in a spherically symmetric, expanding envelope, we initially consider monochromatic X-rays, deferring the discussion of energy dependence to the next section. Let us first define the usual (p, z)-coordinates in such a way that z is a coordinate along a ray, and p is the "impact parameter" or minimum radial distance of the ray from the origin. From a formal solution of the transfer equation for X-rays emitted at a radius $r = (p^2 + z^2)^{1/2}$ with emissivity $\eta(r)$, the specific intensity observed at large radii ($z \to \infty$) is

$$I_p = \int_{-\infty}^{\infty} \eta(r) e^{-\tau(p,z)}\, dz \ . \tag{1}$$

The total X-ray luminosity is then given by integration over all rays

$$L_X = 8\pi^2 \int_0^{\infty} I_p\, p\, dp \ . \tag{2}$$

Here the ray optical depth is of the form

$$\tau(p, z) = \int_z^{\infty} \kappa_X[r(p, z')]\rho[r(p, z')]\, dz' \ , \tag{3}$$

where ρ is the mass density, and κ_X is the X-ray absorption cross section per unit mass. We note that the opacity arises in relatively cool, unshocked portions of the wind and is due primarily to K-shell bound-free transitions in He, C, N, O, Ne, Na, Mg, and Si.

For an instability-generated shock model, X-ray emission is only expected once the wind has reached a substantial fraction ($\gtrsim 50\%$) of the terminal speed v_∞, implying that the radial variation of mean wind density is within an order unity factor of that for a *constant* velocity (Owocki 1994; Feldmeier 1995). For simplicity, let us thus consider the case of expansion at a constant velocity v_∞ (but see Appendix A for a treatment of a beta velocity law). Moreover, since ionization fractions are also fairly constant beyond about $0.5v_\infty$ (MacFarlane, Cohen, & Wang 1994), we assume also a radially constant X-ray mass-absorption coefficient, κ_X. The radial optical depth is then given simply by

$$\tau(0, r) = \frac{\kappa_X \dot{M}}{4\pi v_\infty} \int_r^{\infty} \frac{dr'}{r'^2} = \frac{R_1}{r} \ , \tag{4}$$

where $\dot{M}$ is the mass-loss rate, and

$$R_1 \equiv \frac{\kappa_X \dot{M}}{4\pi v_\infty} \tag{5}$$

defines the radius of unit radial optical depth; i.e., $\tau(0, R_1) \equiv 1$. For nonradial ($p \neq 0$) rays, we obtain

$$\tau(p, z) = R_1 \int_z^{\infty} \frac{dz'}{p^2 + z'^2} = \frac{R_1}{p} \arccos\left(\frac{z}{\sqrt{p^2 + z^2}}\right)$$

$$= \frac{R_1}{p}\, \theta(p, z) \ , \tag{6}$$

where θ is the angle between the $+z$ ray direction and an outward radius vector. This suggests it would be convenient to recast the intensity integral (eq. [1]) in terms of this angle:

$$I_p = p \int_0^{\pi} \frac{\eta[r(p, \theta)]}{\sin^2\theta\, e^{R_1\theta/p}} d\theta \ . \tag{7}$$

To proceed, we next note that X-ray emission arises primarily from two-body processes, recombination and collisional excitation, and thus has a volume emissivity η (ergs s^{-1} cm^{-3} sr^{-1}) that is proportional to the square of the density:

$$\eta(r) = \xi C_s\, f_m \rho^2(r) = \xi C_s^2\, f_v \rho^2(r) \ , \tag{8}$$

where f_m is the *mass* fraction, or mass filling factor, of ambient wind that is X-ray–emitting, and $C_s \equiv \rho_s/\rho$ is a factor to correct for any differences in the density ρ_s of shocked material relative to the ambient wind density ρ (which assumes a smooth wind, given by $\rho \equiv \dot{M}/4\pi r^2 v$). We note that the factor C_s accounts for both the postshock compression and the deviations of the preshock density from the ambient wind density. The mass filling factor, f_m, is related to the volume filling factor by $f_v = f_m/C_s$. The emission coefficient ξ (ergs cm^3 s^{-1} g^{-2}) is related to the commonly used cooling function Λ (ergs s^{-1} cm^3; e.g., Raymond & Smith 1977) by $\xi = \Lambda/4\pi\mu_e\mu_p$, where μ_e and μ_p are the mean mass per electron and proton, respectively. Under typical stellar wind conditions, ξ is independent of density (at least when considered at the coarse spectral resolution associated with current X-ray detectors) and depends mainly on the electron temperature in the postshock region. Assuming for now that the factor $\xi C_s^2 f_v$ is spatially constant, the intensity integral (eq. [7]) can be rewritten and evaluated as

$$I_p = \frac{\xi C_s^2 f_v}{p^3} \left(\frac{R_1}{\kappa_X}\right)^2 \int_0^{\pi} \sin^2\theta\, e^{-R_1\theta/p} d\theta$$

$$= 2\xi C_s^2 f_v \frac{R_1}{\kappa_X^2} \left(\frac{1 - e^{-\pi R_1/p}}{R_1^2 + 4p^2}\right) . \tag{9}$$

Application to the luminosity integral (eq. [2]) then yields

$$L_X = 4\pi^2 \xi C_s^2 f_v \frac{R_1}{\kappa_X^2} \int_0^\infty \frac{1 - e^{-2\pi x}}{x(1+x^2)} dx \approx 9.76\pi^2 \xi C_s^2 f_v \frac{R_1}{\kappa_X^2}$$

$$= 2.44\pi \frac{\xi C_s^2 f_v}{\kappa_X} \frac{\dot{M}}{v_\infty} , \quad (10)$$

where the approximate equality follows from a direct numerical evaluation of the integral. Note that, although the wind volume emission varies as the density squared, the X-ray luminosity escaping the wind scales only *linearly* with the density parameter $\dot{M}/v_\infty$ because of the effect of wind attenuation.

2.2. *Exospheric Approximation for Power-Law Radial Emission*

It is of interest to compare this numerical result with the heuristic formula from an "exospheric approximation" (Cohen et al. 1996) that estimates the X-ray luminosity from the volume integral of the outward (i.e., radiated into 2π sr) emission beyond the radius with unit radial optical depth:

$$L_X \approx 8\pi^2 \int_{R_1}^\infty \eta(r) r^2 \, dr = \frac{2\pi \xi C_s^2 f_v \dot{M}}{\kappa_X v_\infty} , \quad (11)$$

where the latter equality follows from straightforward analytic integration. The rough agreement with the numerical result (eq. [10]) suggests that this simple exospheric formula should be quite useful for estimating L_X in more complicated cases for which the required integrals are difficult to evaluate.

Therefore, let us next estimate L_X for the somewhat more general case when the factor $\xi C_s^2 f_v$ varies as a power law beyond some lower boundary radius R_0 for X-ray emission:

$$\eta(r) = \rho^2 (\xi C_s^2 f_v)_0 \left(\frac{r}{R_0}\right)^s , \quad r > R_0 , \quad (12a)$$

$$\eta(r) = 0 , \quad r < R_0 , \quad (12b)$$

where $(\xi C_s^2 f_v)_0$ is the emission factor at $r = R_0$. Unlike for the special case $R_0 = R_*$ and $s = 0$ considered above, an exact evaluation for L_X would now generally require a numerical evaluation of a double integral over p and z. However, application of the exospheric formula (eq. [11]) readily yields an approximate analytic scaling law for the X-ray luminosity:

$$L_X \approx \frac{(\xi C_s^2 f_v)_0}{2(1-s)} \left(\frac{\dot{M}}{v_\infty}\right)^2 R_0^{-s} [\max(R_0, R_1)]^{s-1} . \quad (13)$$

We note parenthetically that this can be recast as a fitting formula:

$$L_X \approx \frac{(\Lambda C_s^2 f_v)_0}{2(1-s)} \mathrm{EM}_w \left[\frac{R_0}{\max(R_0, R_1)}\right]^{1-s} , \quad (14)$$

where $\mathrm{EM}_w = \int_{R_0}^\infty n^2 \, dV \, ol$ is the total wind emission measure above R_0. Alternatively, we can express this in terms of the basic stellar wind parameters:

$$L_X \approx \frac{(\xi C_s^2 f_v)_0}{2(1-s) R_0} \left(\frac{4\pi R_0}{\kappa_X}\right)^{1-s} \left(\frac{\dot{M}}{v_\infty}\right)^{1+s} ,$$

$$R_0 < R_1 \text{ (optically thick)} , \quad (15a)$$

$$L_X \approx \frac{(\xi C_s^2 f_v)_0}{2(1-s) R_0} \left(\frac{\dot{M}}{v_\infty}\right)^2 , \quad R_0 > R_1 \text{ (optically thin)} . \quad (15b)$$

Equations (15a) and (15b) represent the X-ray luminosity for the "thick" and "thin" wind cases, respectively. Note that the luminosity now scales with $(\dot{M}/v_\infty)^2$ for the thin wind but only with $(\dot{M}/v_\infty)^{1+s}$ for the thick wind.

We reiterate that these results have all been derived for monochromatic X-rays. We will see in § 3 that a given stellar wind can be optically thick at some energies and optically thin at others, leading to spectral structure based on the energy dependence of the X-ray attenuation.

2.3. *Relation to Wind Scaling Laws*

The above simple analysis illustrates that the most direct scaling of the X-ray luminosity should be with wind density and not, as has generally been inferred empirically, with the bolometric luminosity. Thus let us next consider whether this inferred scaling could be explained through secondary scaling of wind density with luminosity. Within the standard Castor, Abbott, & Klein (1975, hereafter CAK) theory for line-driven winds, the mass loss is predicted to scale as

$$\dot{M} \sim L_{\mathrm{Bol}}^{1/\alpha'} M_{\mathrm{eff}}^{1-1/\alpha'} , \quad (16)$$

where M_{eff} is the effective stellar mass [$M_{\mathrm{eff}} = M_*(1 - \Gamma_{\mathrm{Edd}})$], and $\alpha' = \alpha - \delta$ is a combination of the two line parameters, α and δ defined by CAK and Abbott (1982), which, respectively, describe the distribution of line opacity and its dependence on ionization level.

As first noted by Kudritzki, Lennon, & Puls (1995), this theoretical scaling is in good general accord with an empirically derived "wind-momentum-luminosity" relation,

$$\dot{M} v_\infty R_*^{1/2} \sim L_{\mathrm{Bol}}^{1/\alpha'} , \quad (17)$$

wherein the connection with the CAK mass-loss formula (eq. [16]) follows from the scaling of the wind terminal speed with the surface escape speed,

$$v_\infty \sim \sqrt{M_{\mathrm{eff}}/R_*} , \quad (18)$$

which is a well-known theoretical (CAK; Pauldrach, Puls, & Kudritzki 1986) and observational (e.g., Lamers, Snow, & Lindholm 1995) result. For O supergiants, the extensive analysis by Puls et al. (1996) empirically obtained a wind-momentum-luminosity relation with a slope implying $\alpha' = 0.57$, which thus gives

$$\frac{\dot{M}}{v_\infty} \sim \frac{L_{\mathrm{Bol}}^{1.75} R_*^{0.5}}{M_*(1 - \Gamma_{\mathrm{Edd}})} . \quad (19)$$

The dependence on the Eddington factor is significant only for stars with very high luminosities. Between an early-B star like λ Sco and an O supergiant like ζ Pup, $(1 - \Gamma_{\mathrm{Edd}})$ changes by only a factor of 2, while the bolometric luminosities vary by almost 3 orders of magnitude.

To convert equation (19) to a scaling with luminosity alone, we can ignore the weak dependence on stellar radius, but we may want to allow for a systematic trend between luminosity and mass. For example, from stellar structure theory one expects a quite strong trend, e.g., $L_{\mathrm{Bol}} \sim M_*^{2.5}$, yielding $\dot{M}/v_\infty \sim L_{\mathrm{Bol}}^{1.35}$. The observed $L_X \sim L_{\mathrm{Bol}}$ relation would then be reproduced by the optically thick wind scaling relation in equation (15b) if $s \approx -0.25$.

By contrast, if we simply ignore any systematic trend between mass and luminosity, the observed $L_X \sim L_{Bol}$ relation would be reproduced by a filling-factor index $s \approx -0.40$. Either scaling is qualitatively consistent with detailed numerical simulations of the line-driven instability, which generally show a gradual drop-off in X-ray production with radius beyond the point where strong shocks begin to form in the wind. But overall it seems that, with such a wind-based model for X-ray emission, connection with the observed $L_X \sim L_{Bol}$ is inherently indirect, requiring a rather specialized cancellation between the wind emission and absorption.

Finally, we note that for lower density winds that are optically thin to X-rays, the X-ray luminosity becomes independent of s, scaling as

$$L_X \sim \left(\frac{\dot{M}}{v_\infty}\right)^2 \sim L_{Bol}^{2.7} \text{ or } L_{Bol}^{3.5} , \tag{20}$$

where the two scalings depend on whether one includes or ignores the systematic variation of luminosity with mass. Either form is in general accord with empirically inferred X-ray scalings, which show that the dependence of X-rays on bolometric luminosity becomes much steeper around early-B stars, corresponding roughly to where the winds are becoming optically thin (Cohen, Cassinelli, & MacFarlane 1997).

3. ENERGY DEPENDENCE

3.1. *Power-Law Absorption and Emission*

All of the above analysis is for monochromatic X-rays. However, current instruments (e.g., *Einstein*, *ROSAT*, and *ASCA*) are sensitive to X-rays over almost 2 orders of magnitude in energy and, even with their quite modest spectral resolutions, have provided some basic information about the spectral energy distributions of X-rays in hot stars. So let us now consider the energy dependence of the absorption and emission and of the resulting luminosity spectrum. Given the modest energy resolution of X-ray observations to date, we focus here on the broadband spectral properties. The X-ray absorption, apart from several prominent K-shell edges, can be fitted roughly by a power law in energy:

$$\kappa_X(E_X) \approx \frac{\kappa_{X0}}{E_X^a} . \tag{21}$$

Hillier et al. (1993) find, for ζ Pup (O4 If), that $a \approx 2$ in layers where helium remains doubly ionized, and that $a \approx 2.8$ where it has recombined to He^+. For ϵ CMa (B2 II), detailed calculations give $a \approx 1.8$ between 100 eV and 1 keV (Cohen et al. 1996). This energy dependence of opacity means a given wind can be optically thick at some energies and optically thin at others. By setting $R_1 = R_0$, we can derive a critical energy,

$$E_1 = \left(\frac{\kappa_{X0}\dot{M}}{4\pi v_\infty R_0}\right)^{1/a} , \tag{22}$$

that separates the parts of the spectrum for which the wind is optically thick ($E_X < E_1$) from those for which the wind is optically thin ($E_X > E_1$).

To derive the form of the luminosity spectrum, one must specify the energy dependence of emission as well as the absorption. For simplicity, let us again assume that the emissivity has a power-law energy dependence:

$$\xi(E_X) = \frac{\xi_*}{E_X^b} , \tag{23}$$

which means that equation (12a) can be written as $\eta = \rho^2(\xi_* C_s^2 f_v)_0 E_X^{-b}(r/R_0)^s$. In Appendix B we show a comparison of this simple, smooth emissivity model with detailed numerical simulations of collisional equilibrium plasmas. This comparison shows that at the low resolution of current instruments, the line-dominated spectra are surprisingly well approximated by a smooth function such as equation (23), with a power-law spectrum being produced by a power-law temperature distribution. The luminosity spectrum is then given by

$$\frac{dL_X}{dE_X} = L_1\left(\frac{E_X}{E_1}\right)^{a(1-s)-b} , \quad E_X < E_1 , \tag{24a}$$

$$\frac{dL_X}{dE_X} = L_1\left(\frac{E_X}{E_1}\right)^{-b} , \quad E_X > E_1 , \tag{24b}$$

where the luminosity at the energy at which wind optical depth is unity, $L_1 \equiv L_X(E_1)$, has the form

$$L_1 = \frac{(\xi_* C_s^2 f_v)_0}{2R_0(1-s)}\left(\frac{4\pi R_0}{\kappa_{X0}}\right)^{b/a}\left(\frac{\dot{M}}{v_\infty}\right)^{2-b/a} . \tag{25}$$

While equations (24a) and (24b) are convenient for plotting the spectrum for a given model, we can alternatively write this in a form that more explicitly displays the scalings with stellar parameters:

$$\frac{dL_X}{dE_X} = \frac{(\xi_* C_s^2 f_v)_0}{2R_0(1-s)}\left(\frac{4\pi R_0}{\kappa_{X0}}\right)^{1-s}\left(\frac{\dot{M}}{v_\infty}\right)^{1+s} E_X^{a(1-s)-b} , \quad E_X < E_1 , \tag{26a}$$

$$\frac{dL_X}{dE_X} = \frac{(\xi_* C_s^2 f_v)_0}{2R_0(1-s)}\left(\frac{\dot{M}}{v_\infty}\right)^2 E_X^{-b} , \quad E_X > E_1 , \tag{26b}$$

where, again, equations (26a) and (26b) represent the expressions for the optically thick and optically thin wind domains, respectively (see eqs. [15a] and [15b]).

Using the simple power-law absorption and emission models, the energy dependencies in the two domains have slopes that differ by $a(1-s)$. Furthermore, if $a(1-s) - b > 0$, then $E_X = E_1$ is also the energy of peak flux, and the value of this peak is dictated solely by the *absorption* properties of the wind. Given equation (22), one would expect the observed values of E_1 to vary significantly from low-density B star winds to high-density O star winds. However, although some variation in the peak intensities are seen, it is much less dramatic than this model predicts. In addition, the relative slopes of the optically thin and optically thick parts of observed X-ray spectra are generally seen to differ by much more than $a(1-s)$, given reasonable values of a and s. These trends are shown in Figure 1 for a representative O star (ζ Pup) and a representative early-type B star (λ Sco).

It is thus apparent that a universal power-law emissivity function is too simple an assumption. An obvious problem with this functional description is that it implies the presence of plasma having an arbitrarily high temperature. It therefore seems appropriate to consider a truncation to the

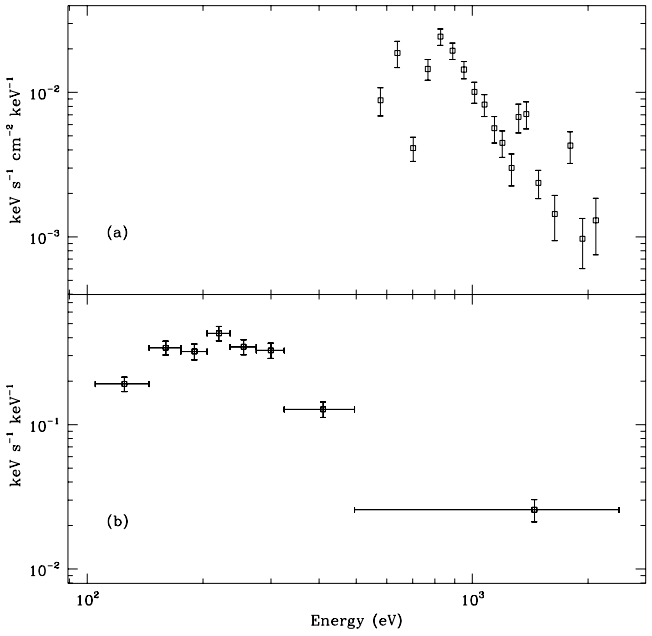

FIG. 1.—(*a*) BBXRT (detector A) spectrum of ζ Pup (O4 If) taken from Corcoran et al. (1993). This spectrum has been "unfolded" so as to correct for the energy-dependent sensitivity of the detector. Note that the peak flux is near 0.7 keV once the oxygen K-edge feature near this energy is corrected for. Given the parameters of ζ Pup ($\dot{M} = 5 \times 10^6\ M_\odot\ \mathrm{yr}^{-1}$, $v_\infty = 2.2 \times 10^3\ \mathrm{km\ s}^{-1}$, $R_* = 1.3 \times 10^{12}$ cm), however, we find a value of $E_1 \approx 2$ keV. Note also that the power-law indices of the slopes of the low- and high-energy portions of the spectrum differ by at least six. The *ROSAT* PSPC spectrum of λ Sco (B1.5 IV) (*b*) has a peak energy (corresponding to E_1) that is in much better agreement with the predicted value of 0.1 keV. The slightly higher observed peak value is entirely consistent with the finding that the mass-loss rates of B stars have been systematically underestimated (Cohen et al. 1997).

power-law emissivity introduced in equation (23) that corresponds roughly to the maximum shock energy in the wind. We therefore modify the emissivity as

$$\xi(E_X) = \frac{\xi_*}{E_X^b}\, e^{-E_X/E_{\max}}\ , \tag{27}$$

where $E_{\max}$ is the maximum plasma temperature, corresponding to the maximum shock energy. The luminosity spectrum is now given by

$$\frac{dL_X}{dE_X} = L_1\left(\frac{E_X}{E_1}\right)^{a(1-s)-b} e^{-E_X/E_{\max}}, \quad E_X < E_1\ , \tag{28a}$$

$$\frac{dL_X}{dE_X} = L_1\left(\frac{E_X}{E_1}\right)^{-b} e^{-E_X/E_{\max}}, \qquad E_X > E_1\ , \tag{28b}$$

where L_1 has the same definition as before. The exponential cutoff in this model brings the luminosity spectrum more in line with the data shown in Figure 1, as well as that for most other OB stars.

With this general expression for the X-ray spectra, one sees that there are two different types of spectra that can occur. If $E_{\max} > E_1$ then the high-energy falloff of the spectrum occurs above E_1, where the spectrum would be decreasing as a power law already. Like the simple power-law expression model, this spectrum has a peak determined by E_1. Effectively, then, the main change is to cause a much steeper high-energy falloff in the spectrum. However, if $E_{\max} < E_1$, then the peak in the spectrum is at a softer energy than it otherwise would have been (at an energy dictated by $E_{\max}$ rather than E_1), and the falloff in the spectrum with increasing photon energy occurs that much sooner.

When O star X-ray data are fitted with two-temperature models (e.g., Hillier et al. 1993), the higher temperature component tends to be approximately 5×10^6 K, rarely exceeding 10^7 K. Even for the cooler B stars, the highest temperature component derived from model fitting is roughly 5×10^6 K (Cassinelli et al. 1994), indicating that $E_{\max}$ should be relatively constant for hot stars, with a value near 0.5 keV. This is in contrast to the values of E_1, which vary by more than an order of magnitude from mid-B to early-O stars. Therefore, which of these two cases applies to a given star depends primarily on the value of E_1, which is governed largely by the mass-loss rate. The case with $E_{\max} < E_1$ is thus appropriate to O stars, with their optically thick winds, while the case with $E_{\max} > E_1$ is relevant for B stars, with their thinner winds. For these low-density winds, the peak energy in the spectrum is determined by the value of E_1, whereas for the higher density, optically thick winds, the peak of the spectrum is relatively constant at the universal value of $E_{\max} \approx 0.5$ keV.

3.2. *The L_X/L_{Bol} Scaling Relation from the Full Spectrum*

With the parameterization of the energy dependence of wind attenuation and wind emission introduced in the previous subsection, we can return to the explanation for the scaling relationship discussed in § 2.3. Because the O stars and early-B stars for which the L_X/L_{Bol} scaling holds have optically thick winds with $E_{\max} < E_1$, the optically thin portion of the wind ($E_X > E_1$) contributes negligibly to the overall X-ray luminosity, and we therefore can consider only the optically thick expression, given by the equation (28a). Furthermore, because of the negligible contribution of the high-energy portion of the spectrum, we can carry out the integration over all energies without significantly affecting the result. The total X-ray luminosity emergent from a hot star wind in this model is then given by

$$\begin{aligned} L_X &\approx \frac{(\xi_*\, C_s^2\, f_v)_0}{2R_0^s(1-s)}\left(\frac{4\pi R_0}{\kappa_{X0}}\right)^{1-s}\left(\frac{\dot{M}}{v_\infty}\right)^{1+s} \\ &\quad \times \int_0^\infty E_X^{a(1-s)-b}\, e^{-E_X/E_{\max}}\, dE_X \\ &= \frac{(\xi_*\, C_s^2\, f_v)_0}{2R_0^s(1-s)}\left(\frac{4\pi R_0}{\kappa_{Xo}}\right)^{1-s}\left(\frac{\dot{M}}{v_\infty}\right)^{1+s} \\ &\quad \times E_{\max}^{1+a(1-s)-b}\Gamma(a-as-b)\ . \end{aligned} \tag{29}$$

This expression preserves the $L_X \sim (\dot{M}/v_\infty)^{1+s}$ dependence, which yields $L_X \sim L_{Bol}$ with $s \approx -0.25$ or $s \approx -0.4$, as we derived in § 2.3 for monochromatic X-rays. We note that this analysis holds only for the optically thick winds that correspond to O stars, which have $L_X/L_{Bol} \approx 10^{-7}$.

The relationship for monochromatic optically thin winds, $L_X \sim (\dot{M}/v_\infty)^2$, is also consistent with the energy-dependent treatment, so long as E_1 is below the soft edge of the instrumental bandpass. Otherwise the observed spectrum has significant contributions from both an optically thin power-law region and an optically thick power-law region. In this hybrid case, the dependence of the X-ray luminosity on the bolometric luminosity is complicated and falls somewhere between the linear dependence of the thick winds and the much steeper dependence of the thin winds. This would

cause a less discontinuous falloff in the L_X/L_{Bol} relationship than is inferred from the monochromatic analysis in § 2.3.

4. CONCLUSIONS

Despite its approximate nature, the analysis described here provides a useful initial framework for examining the interplay among the basic processes of X-ray emission and absorption that determine the observed X-ray spectra from a hot-star wind.

Some of the main points are as follows:

1. The simple procedure (see eq. [11]) of including only the X-ray emission above the radius R_1 of unit optical depth (the exospheric approximation) provides an accurate means to account for X-ray attenuation effects. A key aspect of this approximation is the assumption that $v \approx v_\infty$, which is indicated theoretically. If the X-rays are formed deeper in the wind, then this constant-velocity approximation will underestimate the X-ray luminosity, but in Appendix A we estimate that the error is generally no more than about 50%.

2. For optically thin winds, the X-ray luminosity increases as $(\dot{M}/v_\infty)^2$, as would be expected based on the density-squared sensitivity of the thermal emission processes. However, the dependence of the X-ray luminosity on wind density is less steep in the case of optically thick winds, with $L_X \sim (\dot{M}/v_\infty)^{1+s}$, where the X-ray filling factor has a power-law radial dependence, $f \sim r^s$.

3. Indeed, the natural scaling of the X-ray luminosity in hot-star winds is with the wind density parameter, $\dot{M}/v_\infty$, and not with stellar parameters such as the bolometric luminosity.

4. However, if one introduces a radial power-law scaling of the filling factor, then the observed $L_X \sim L_{Bol}$ relation can be recovered with a value of $s \approx -0.25$ to $s \approx -0.4$ for the radial power-law index.

5. The energy dependence of the unit-optical-depth radius R_1 can play an important role in the shape of the energy spectrum. Indeed, in the simple shock model presented here, the peak of the spectrum occurs at the energy E_1 for which X-rays become optically thin at the initial shock onset radius R_0, as long as the emissivity does not begin to fall off rapidly at energies below E_1. This condition should be satisfied for the low-density B star winds. However, for O star winds, the peak of the spectrum is governed by the high-energy cutoff in the shock strength distribution.

6. The X-rays observed by satellite telescopes are, especially for stars with optically thick winds, only a fraction of the total X-ray production. A significant amount of the X-ray production is absorbed by the optically thick winds of these stars. In addition, a significant amount of the total generated X-ray emission may fall outside of the observational bandpasses, especially in the very soft X-ray and EUV.

Future work will apply the principles illuminated here to the interpretation of more fundamental, numerical simulations of X-ray emission from instability-generated shocks, to a detailed analysis of shock heating and cooling mechanisms, and to the interpretation of observational data. This will help clarify the strengths and weaknesses of the wind instability paradigm for explaining the observed X-ray spectra and scaling relations.

This research was supported in part by NASA grant NAG 5-3530 to the Bartol Research Institute at the University of Delaware.

APPENDIX A

EXOSPHERIC MODEL WITH A BETA VELOCITY LAW

Although there is good reason to believe that the X-ray production in hot-star winds occurs primarily in regions of the wind where the velocity is close to the terminal velocity, it is possible to relax this assumption and still analytically solve for the X-ray luminosity under the exospheric approximation (eq. [11]) if the filling factor is radially constant.

The exospheric approximation is given by

$$L_X \approx 8\pi^2 \int_{R_1}^{\infty} \eta(r)\, r^2\, dr\ , \tag{A1}$$

where the emissivity $\eta \sim \rho^2$, and R_1 is the radius at which the radial optical depth is unity, $\tau(0, R_1) \equiv 1$. For a "beta" velocity law of the form

$$v(r) = v_\infty(1 - R_*/r)^\beta\ , \tag{A2}$$

the radial optical depth is given by the integral

$$\tau(0, r) = \frac{\kappa_X \dot{M}}{4\pi v_\infty} \int_r^{\infty} \frac{dr'}{r'^2(1 - R_*/r')^\beta}\ , \tag{A3}$$

which, through a variable substitution $y = (1 - R_*/r)$, can be readily evaluated as

$$\tau(0, r) = \frac{\kappa_X \dot{M}}{4\pi v_\infty R_*(1 - \beta)} \left[1 - \left(\frac{1 - R_*}{r}\right)^{1-\beta}\right]. \tag{A4}$$

Setting $\tau = 1$ leads to a new expression for the unit-optical-depth radius,

$$R_1^{\text{beta}} = R_* \left\{1 - \left[1 - \frac{R_*(1 - \beta)}{R_1^0}\right]^{1/(1-\beta)}\right\}^{-1}\ , \tag{A5}$$

where $R_1^0 \equiv \kappa_X \dot{M}/4\pi v_\infty$ is the previous result for a constant velocity flow, which simply represents the special case $\beta = 0$.

Making the same change of variables in the exospheric expression for the X-ray luminosity and using the newly defined lower limit of integration, $R_1^{\rm beta}$, one finds

$$L_X^{\rm beta} = \frac{\xi C_s^2 f_v \dot{M}^2}{2R_*(1-2\beta)v_\infty^2}\left\{1-\left[1-\frac{R_*(1-\beta)}{R_1^0}\right]^{(1-2\beta)/(1-\beta)}\right\}. \quad \text{(A6)}$$

Scaled by the constant-velocity exospheric expression (eq. [11]), this can be cast as a correction factor:

$$\frac{L_X^{\rm beta}}{L_X} = \frac{R_1^0}{R_*(1-2\beta)}\left\{1-\left[1-\frac{R_*(1-\beta)}{R_1^0}\right]^{(1-2\beta)/(1-\beta)}\right\}. \quad \text{(A7)}$$

Note that as R_1^0/R_* approaches infinity, $L_X^{\rm beta}/L_X$ approaches unity. Furthermore, for $\beta = 0.8$ if $R_1 = 2R_*$, then $L_X^{\rm beta}/L_X \approx 1.25$. Choosing an R_1^0 that gives $R_1^{\rm beta} = 1.5R_*$, which seems a reasonable minimum radius for onset of instability-generated X-rays, $L_X^{\rm beta}$ is just over 50% greater than L_X.

APPENDIX B

COMPARISON OF POWER-LAW EMISSION SPECTRA WITH NUMERICAL MODELS

Given that the optically thin, thermal emission expected from the shock-heated regions of hot-star winds is dominated by lines (e.g., Raymond & Smith 1977; Mewe, Groenenschild, & van den Oord 1985), we may ask how well the smooth power-law models we have assumed in this paper represent the true spectra. We thus created a series of collisional equilibrium spectral models using the MeKaL code (Mewe, Kaastra, Liedahl 1995) and assuming B star abundances (Geis & Lambert 1992). These are power-law differential emission models of the form $(d\ \mathrm{EM}/dT) \sim 1/T^c$ that are constructed from a superposition of multiple isothermal models. The individual isothermal models used to make the power-law differential emission models have temperatures in the interval $5.0 \leq \log T(\mathrm{K}) \leq 7.7$. The spectra were calculated in the range 15–2500 eV. Although 100 eV is generally taken to be the lower bound of the X-ray bandpass, significant emission occurs at lower energies, even for very hot plasma. We have compared these single power-law temperature distribution models with the single power-law spectral models described by equation (23).

Currently, the best spectral resolution available from space-based observatories is $\lambda/\Delta\lambda \approx 20$ from BBXRT and *ASCA*. We therefore binned the detailed models at slightly better than this resolution and fitted the resulting spectra with single power laws, $\xi \sim E_X^{-b}$. Three examples of this exercise are shown in Figure 2. The power-law assumption is seen to be quite good. Reasonable χ^2 values result from these fits if statistical uncertainties of only a factor of 2–3 are assumed for each bin. It should

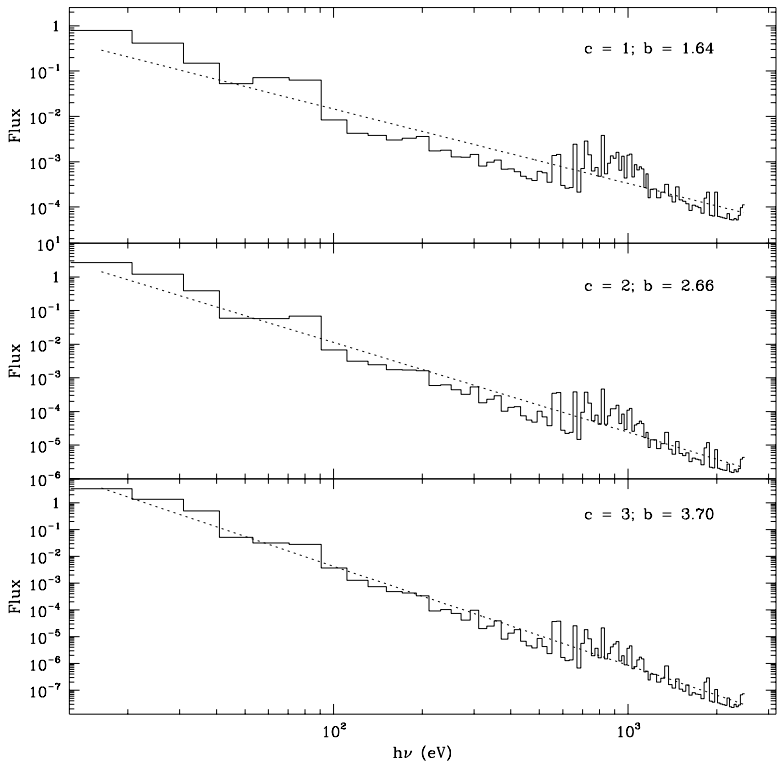

FIG. 2.—Temperature power-law spectral models (*solid lines*) calculated from the MeKaL code shown along with the power-law spectral fits (*dotted lines*). The best-fit power-law spectral indices (*b*) are indicated along with the differential emission measure slope used in making the models (*c*).

be kept in mind that the actual resolution of most available X-ray data sets is significantly worse than the binning of these models indicate, so that the observed data are, in fact, even more well described by power laws.

There are several interesting things to note from this exercise. First, the global structure in these model spectra are dominated by the emission bump centered near 0.8 keV. This feature is due to thousands of iron L-shell emission lines. Second, a very significant fraction of the flux emerges not in the soft X-ray but actually in the EUV, below 100 eV. Although this radiation is very significant (not least because of the role it plays in determining the wind excitation and ionization conditions), it has been directly observed in only one hot star, ϵ CMa (Cohen et al. 1996). Finally, the best-fit spectral power-law slopes are generally steeper than the power-law slopes of the differential emission measure (plasma temperature) distributions by roughly 0.7. This factor is a reflection of the fact that in the temperature range $10^5 < T < 10^7$, hotter plasma emits less efficiently than cooler plasma. Indeed, the slope of the frequency-integrated cooling curve between the temperatures of 10^5 and 10^7 K (e.g., Raymond, Cox, & Smith 1976) is very close to the value 0.7.

REFERENCES

Abbott, D. A. 1982, ApJ, 263, 723
Baade, D., & Lucy, L. B. 1987, A&A, 178, 213
Cassinelli, J. P., Cohen, D. H., MacFarlane, J. J., Sanders, W. T., & Welsh, B. Y. 1994, ApJ, 421, 705
Cassinelli, J. P., & Olson, G. L. 1979, ApJ, 229, 304
Cassinelli, J. P., Olson, G. L., & Stalio, R. 1978, ApJ, 220, 573
Cassinelli, J. P., & Swank, J. H. 1983, ApJ, 271, 681
Castor, J. I., Abbott, D. C., & Klein, R. I. 1975, ApJ, 195, 157 (CAK)
Chlebowski, T., Harnden, F. R., Jr., & Sciortino, S. 1989, ApJ, 341, 427
Cohen, D. H., Cassinelli, J. P., & MacFarlane, J. J. 1997, ApJ, 487, 867
Cohen, D. H., Cooper, R. G., MacFarlane, J. J., Owocki, S. P., Cassinelli, J. P., & Wang, P. 1996, ApJ, 460, 506
Corcoran, M. F., et al. 1993, ApJ, 412, 792
Feldmeier, A. 1995, A&A, 299, 523
Feldmeier, A., Kudritzki, R.-P., Palsa, R., Pauldrach, A. W. A., & Puls, J. 1997a, A&A, 320, 899
Feldmeier, A., Puls, J., & Pauldrach, A. W. A. 1997b, A&A, 322, 878
Geis, D. R., & Lambert, D. L. 1992, ApJ, 387, 673
Harnden, F. R., Jr., et al. 1979, ApJ, 234, L51
Hillier, D. J., Kudritzki, R. P., Pauldrach, A. W. A., Baade, D., Cassinelli, J. P., Puls, J., & Schmitt, J. H. M. M. 1993, A&A, 276, 117
Kudritzki, R. P., Lennon, D., & Puls, J. 1995, in Science with the Very Large Telescope, ed. J. Walsh & I. Danziger (Berlin: Springer), 246
Kudritzki, R. P., Palsa, R., Feldmeier, A., Puls, J., & Pauldrach, A. W. A. 1996, in Röntgenstrahlung from the Universe, ed. H. U. Zimmermann, J. Trümper, & H. York (Garching: MPE), 9
Lamers, H. J. G. L. M., Snow, T. P., & Lindholm, D. M. 1995, ApJ, 455, 269
Long, K. S., & White, R. L. 1980, ApJ, 239, L65
Lucy, L. B. 1982, ApJ, 255, 286
Lucy, L. B., & Solomon, P. M. 1970, ApJ, 159, 879
Lucy, L. B., & White, R. L. 1980, ApJ, 241, 300
MacFarlane, J. J., Cohen, D. H., & Wang, P. 1994, ApJ, 437, 351
MacFarlane, J. J., Waldron, W. L., Corcoran, M. F., Wolff, M. J., & Wang, P. 1993, ApJ, 419, 813
MacGregor, K. B., Hartmann, L., & Raymond, J. C. 1979, ApJ, 231, 514
Mewe, R., Gronenschild, E. H. B. M., & van den Oord, G. H. J. 1985, A&AS, 62, 197
Mewe, R., Kaastra, J. S., & Liedahl, D. A. 1995, Legacy, 6, 16
Nordsieck, K. H., Cassinelli, J. P., & Anderson, C. M. 1981, ApJ, 248, 678
Owocki, S. P. 1994, Ap&SS, 221, 30
Owocki, S. P., Castor, J. I., & Rybicki, G. B. 1988, ApJ, 335, 914
Owocki, S. P., & Rybicki, G. B. 1984, ApJ, 284, 337
———. 1985, ApJ, 299, 265
Pallavicini, R., Golub, L., Rosner, R., Vaiana, G. S., Ayres, T., & Linsky, J. L. 1981, ApJ, 248, 279
Pauldrach, A. W. A., Puls, J., & Kudritzki, R.-P. 1986, A&A, 164, 86
Puls, J., et al. 1996, A&A, 305, 171
Raymond, J. C., Cox, D. P., & Smith, B. W. 1976, ApJ, 204, 290
Raymond, J. C., & Smith, B. W. 1976, ApJS, 35, 419
Seward, F. D., Forman, W. R., Giacconi, R., Griffiths, R. E., Harnden, F. R., Jr., Jones, C., & Pye, J. P. 1979, ApJ, 234, L55
Waldron, W. L. 1984, ApJ, 282, 256